A study of the complex dynamics of dendrite solidification coupled to structural mechanics.

A study of the complex dynamics of dendrite solidification coupled to structural mechanics.

P Soar, A Kao, G Djambazov and K A Pericleous

Centre for Numerical Modelling and Process Analysis, University of Greenwich, Old Royal Naval College, Park Row, London, SE109LS, United Kingdom

E-mail: P.Soar@gre.ac.uk

Abstract. The impact of structural mechanics is often overlooked when modelling the solidification of dendritic microstructures, despite experimental observations that the interaction between these processes can be a factor leading to the development of crystal mosaicity throughout the microstructure which can itself lead to more serious defects. When considered at all, the structural mechanical behaviour of columnar dendrites is often considered as being analogous to a cantilever beam both in interpretations of experimental results and in existing numerical modelling. While this is not an unreasonable assumption when considering a dendrite in isolation, this is a scenario that infrequently occurs. In this paper a parametric study is presented using a Cellular Automata solidification solver coupled to a Finite Volume Structural Mechanics solver. These results highlight the complex non-linear behaviour that arises when considering dendrite interaction, demonstrating the significantly different microstructures that can be obtained by varying only the force experienced by the system.

1. Introduction

Structural mechanical effects have been widely observed in experimental results as one of the factors than can influence the development of solidifying dendritic microstructures, with examples identifying structural effects as the root cause of dendrites observed bending [1], fracturing [2] and leading to the formation of serious casting defects such as slivers [3]. Even in less extreme instances, the structural mechanical influences on the microstructure development can be observed in more gradual dendrite misorientations [4], which are not uncommon in any dendritic microstructure and can lead to the substructures of misoriented dendrites to occur even in single crystal castings in a phenomenon known as crystal mosaicity [5].

The interaction between structural mechanics and microstructure solidification is a complex, interdependent process that defies easy characterisation when considering the development of larger systems comprising multiple interacting dendrites. For this reason, when interpreting results the analogy has often been made that a single columnar dendrite behaves in a manner analogous to that of a cantilever beam anchored to either the nucleation site at the edge of the sample [6], by the solidifying interdendritic front [3, 7, 8, 4] or when considering a secondary arm anchored to a primary dendrite trunk [1]. This assumption of beam like behaviour has also been made when modelling the process, where beam models have been used to make assumptions about dendrite fragmentation [2]. Indeed, investigations using the Finite Element Method have shown that while a single dendrite will experience higher stress than a comparable

simple cantilever due to the morphology around the dendrite neck, the behaviour of the modelled dendrite still follows a comparable power law in its behaviour [6].

While the assumption of cantilever beam like behaviour appears appropriate when considering the mechanical behaviour of a single dendrite, this overlooks a great deal of complexity when considering the full solidifying system. There is the issue of in situ observations being difficult for many realistic systems, leading to questions of when during the solidification process deformation occurs, with some experiments positing thermal contraction to cause cantilever beam like deformation of dendrites in an already significantly developed microstructure [3, 8, 4, 9]. In other cases it has been proposed that misorientation can occur near the tips of dendrites which are still in the mushy zone, before having any deformation frozen in place by the advancing solidification of the interdendritic material [7], meaning that the region which is free to deform like a cantilever will remain limited to the length of the mushy zone rather than the total length of the dendrite in question. Even within the mushy zone, the mechanical behaviour of dendrites may be further constrained by the convergence of the secondary arms, which allows load to pass between dendrites [7]. This can potentially lead to regions of high stress where a dendrite deform like a cantilever causing secondary arms to impact [10], while in other cases these impinging secondary arms lead to successive dendrites forming a strip which acts together in a cantilever beam like manner [11].

The impact of structural mechanics is often neglected when numerically modelling the microstructure solidification process, with limited examples of fully coupled modelling [12] and no 3D modelling of the process other than the prior work by the authors [13] where some of the more complex structural behaviours which can only be represented in 3D such as out of plane bending and torsion were investigated. However, in this work these behaviours will not be considered, focussing instead on the relatively simpler case of a constant body force acting perpendicular to the dendrite growth orientation. An experimental example of a system analogous to this case which demonstrated dendrites becoming misoriented in the direction of gravity can be found in figure 1, which was previously compared to an earlier 2D version of this modelling in Soar et al. (2022) [14]. Consequently, a parametric study will be conducted which varies this constant body force to explore how this can cause significant differences in both growth behaviour and final morphology of the dendritic structures, these results will then be used to consider how well the assumption holds that columnar dendrites behave like cantilever beams throughout the simulations.

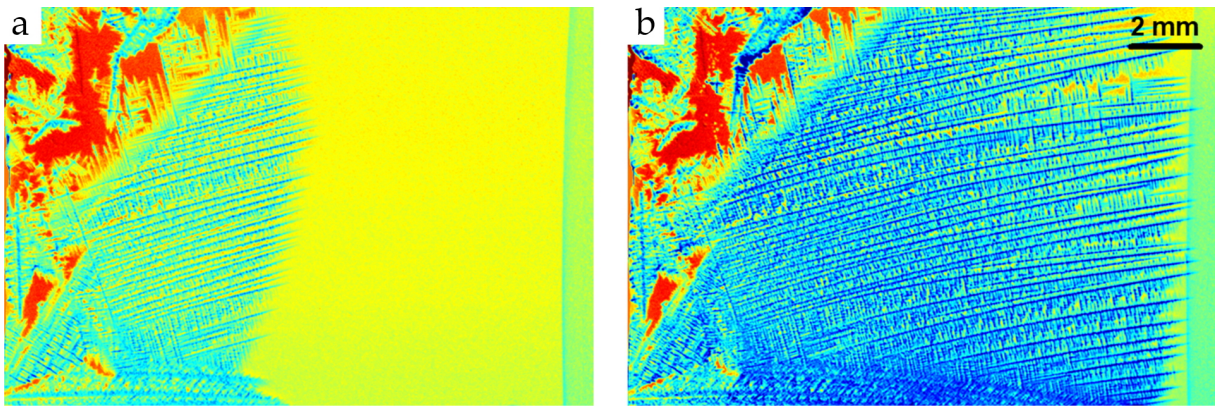

Figure 1: Experimental results from Soar et al. (2022) [14] showing the accumulation of misorientation in columnar dendrites during the solidification of a $Ga - 25wt\%In$ alloy.

2. Methodology

This section will provide a quick summary of the methods used to obtain the results. Other than the problem setup, the numerical modelling used is identical to that presented in previous papers by the authors [14, 13] which provide more in depth descriptions of the methodology used.

The model for microstructure alloy evolution uses a finite difference decentred octahedron Cellular Automata (CA) method based on the Imperial College μMatIC code [15] which has been further developed into the parallel multi-physics code Thermo Electric Solidification Algorithm (TESA) [16]. This solidification method uses the following governing equation for the transient phase change and solute partitioning

$$C_l\,(1-k)\,\frac{\partial \phi_s}{\partial t} = -\nabla\cdot(D_e \nabla C_l) + [1-(1-k)\,\phi_s]\,\frac{\partial C_l}{\partial t}, \tag{1}$$

where C_l and C_s are respectively the liquid and solid concentration, $k = C_l/C_s$ is the partition coefficient, $0 \leq \phi_s \leq 1$ is the solid fraction, D_e is the mass diffusivity and t is time. The diffusive transport of this system is given by

$$\frac{\partial C_e}{\partial t} = \nabla\cdot(D_e \nabla C_l)\,, \tag{2}$$

defining the equivalent concentration as $C_e = (1-\phi_s)\,C_l + \phi_s C_s$. A frozen temperature approximation has been taken with a constant thermal gradient in the primary growth direction and a constant cooling rate. As the system has a Lewis number of approximately 10000, the thermal field drives to quasi-steady equilibrium much faster than the solute allowing this convenient assumption to be made to simplify the system being solved. The equilibrium temperature at the interface given as

$$T_i = T_0 + m_l\,(C_l - C_0)\,, \tag{3}$$

where C_0 is the initial concentration, T_0 is the initial liquidus temperature and m_l is the liquidus slope.

A Linear Elasticity material model has been used to represent the three-dimensional structural mechanical behaviour of the system. This material model requires assumptions that stress and strain are linearly related, that the displacements are 'small' and that there is no yielding behaviour. While these are certainly limiting assumptions that cannot hold for all cases where microstructure solidification is influenced by structural mechanics, they are sufficient for scenarios where the gradient of the displacements, and thereby orientation change, have a larger impact on the microstructure development than the absolute displacements. The displacements are governed by the following three sets of linked partial differential equations which are solved simultaneously using a quasi-stationary Finite Volume solver where the body forces act transiently so that the change in force since the last time step rather than the total force is considered.

$$(\lambda+\mu)\left(\frac{\partial^2 u}{\partial x^2}+\frac{\partial^2 v}{\partial x \partial y}+\frac{\partial^2 w}{\partial x \partial z}\right)+\mu\left(\frac{\partial^2 u}{\partial x^2}+\frac{\partial^2 u}{\partial y^2}+\frac{\partial^2 u}{\partial z^2}\right)+F_x = 0 \tag{4}$$

$$(\lambda+\mu)\left(\frac{\partial^2 v}{\partial y^2}+\frac{\partial^2 u}{\partial y \partial x}+\frac{\partial^2 w}{\partial y \partial z}\right)+\mu\left(\frac{\partial^2 v}{\partial x^2}+\frac{\partial^2 v}{\partial y^2}+\frac{\partial^2 v}{\partial z^2}\right)+F_y = 0 \tag{5}$$

$$(\lambda+\mu)\left(\frac{\partial^2 w}{\partial z^2}+\frac{\partial^2 u}{\partial z \partial x}+\frac{\partial^2 v}{\partial z \partial y}\right)+\mu\left(\frac{\partial^2 w}{\partial x^2}+\frac{\partial^2 w}{\partial y^2}+\frac{\partial^2 w}{\partial z^2}\right)+F_z = 0 \tag{6}$$

where u, v and w are the displacements in x, y and z, F_x, F_y and F_z are the corresponding body forces and μ and λ are the Lamé constants:

$$\lambda = \frac{\eta E}{(1+\eta)(1-2\eta)} \tag{7}$$

$$\mu = \frac{E}{2(1+\eta)} \tag{8}$$

where E and η to be the Young's Modulus and Poisson's ratio of the material respectively. Material properties may vary both spatially and temporally as solidification progresses, allowing the Young's modulus of the dendrites to vary according to a linear relationship with the solid fraction. The impact of thermal contraction has been neglected for the cases examined, with the material properties assumed to be temperature independent. The crystallographic orientation of the dendrites is used as a means of coupling solidification to the structural mechanics, where the displacements are used to alter the local orientation by obtaining three extrinsic rotations θ_x, θ_y and θ_z around their corresponding axes which can be combined into a single 3D orientation change for each computational cell comprising the dendrite, though it should be noted that for the cases examined in this paper the orientation change in the direction of the constant body force (θ_z) is significantly larger and dominates the orientation change behaviour such that any out of plane bending or torsion is negligible.

3. Results

The numerical model has been used to run a parametric study to examine the changing behaviour of a dendrite growing under a constant body force, where all cases in the study are identical other than the magnitude of the body force. The dendrite was seeded on the west wall of a 2mm $\times$ 2mm $\times$ 12mm domain with an initial orientation of $\theta_z = 20^\circ$ and $\theta_x = \theta_y = 0^\circ$ and a constant thermal gradient G along the x axis which cools at a constant rate Q throughout the simulation. Periodic boundaries were used for the North, South, High and Low boundaries so that rather than modelling a single dendrite growing in a 'box', the modelling instead represents a subsection of an infinite field of identical dendrites. Whilst still an idealised scenario, this setup was chosen as it serves to highlight the impact of dendrite interaction as well as preventing interaction with the wall from limiting both the growth and displacement behaviour of the dendrite. All relevant variables related to the material properties and general model setup can be found in table 1, as representative of those used in experiments for solidifying a $Ga - 25wt\%In$ alloy, chosen for easier comparison with earlier work which used this material [14, 13]. The only properties of note are the Young's Modulus (E) and Poisson's Ratio (η), with accurate values for these properties being unclear due to the lack of information in the literature for the mechanical behaviour of semi-solid dendrites, with $\eta = 0.3$ being chosen as a the standard value for the fully solidified alloy while $E = 10$MPa was chosen arbitrarily so as to be low enough to allow significant orientation change to occur during the largest magnitude case examined. It should be noted that as the Young's Modulus and the force are related quantities such any problem with the same ratio of $E : F$ will have identical results, meaning that the results presented can be considered valid for an entire family of solutions using a given ratio.

This study will examine five cases where the constant body force in y is changed, taking the values $F_y = 100$ N/m^3, 1000 N/m^3, 2500 N/m^3, 5000 N/m^3 and 10000 N/m^3, where the body forces in the other directions are fixed as $F_x = F_z = 0$ N/m^3 . These forces act on the solid material only and any other forces that may realistically arise in this scenario are neglected. For the duration of the paper, these five cases will be identified by a number corresponding to what multiple of the initial 100 N/m^3 case, making the examined cases respectively 1, 10, 25, 50 and 100. The simulations for all cases have been run for 250000 timesteps, meaning

the final state of the simulation occurs 1250 seconds after the initial seeding, with this final state for all cases being visible in figure 2. For cases 1 and 10 little visible orientation change has occurred along the length of the dendrite arm, though the cumulative orientation changes throughout the simulation have caused the tip of the dendrite in case 10 to have a significantly different position and orientation to case 1, along with various minor changes in the secondary arm development. There is some clear orientation change across the primary dendrite trunk observable in case 25, with the dendrite orientation flattening off and almost approaching 0° by the end of the simulation, while in case 50 this change is even further exaggerated such that the total orientation at the tip is now clearly negative. By case 100 it becomes difficult making direct comparisons to the other cases due to the impact of the significant misorientation on the morphology of the microstructure, where the tip of the main dendrite arm is approaching an orientation parallel to gravity and being outcompeted by a secondary arm that would likely become a new primary arm if the simulation was continued.

Throughout the simulations the transient behaviour of the orientation change and displacements have also been recorded to see if there are any obvious patterns in growth behaviour to be observed across the different cases. The first structural behaviour examined is the orientation change (such that any values presented are the change relative to the seeded orientation of $\theta_z = 20°$ rather than the current orientation at the tip), where values at regular 50000 timestep intervals the maximum observed orientation change for all cases have been recorded in the left section of table 2, with graphs showing more granular orientation change information from the simulation for easier visual interpretation in figure 3.

The graphs show both the raw values indicating the absolute difference in values in figure 3a and a 'scaled' orientation change in figure 3b for easier comparison of their relative behaviour. In this context 'scaled' means the final observed orientation is divided by the force multiplier corresponding to the case number, which means that if there was a linear relationship between force increase and the orientation change then the orientation change lines for case 1 and all the scaled cases should be identical.

By utilising a combination of the outputs in table 2 and figure 3 some clear patterns in the development of the orientation change emerge. Considering only the simulation up to step $t = 100000$, there appears to be an essentially linear relationship between the force and

Property	**Variable**	**Value**	**Unit**
Density Ga	ρ_{Ga}	6095	kgm^{-3}
Density In	ρ_{In}	7020	kgm^{-3}
Young's Modulus	E	10	MPa
Poisson's Ratio	η	0.3	–
Liquidus Slope	m_l	-2.9375	$\mathrm{K\%wt.}^{-1}$
Partition Coefficient	k	0.5	–
Liquid Mass Diffusivity	D_l	2×10^{-9}	$\mathrm{m}^2\mathrm{s}^{-1}$
Solid Mass Diffusivity	D_s	1×10^{-12}	$\mathrm{m}^2\mathrm{s}^{-1}$
Cooling Rate	Q	0.01	Ks^{-1}
Thermal Gradient	G	1	Kmm^{-1}
Cell Size	Δx	10	µm
Time step	Δt	5	ms

Table 1: Material properties and problem setup used for all cases.

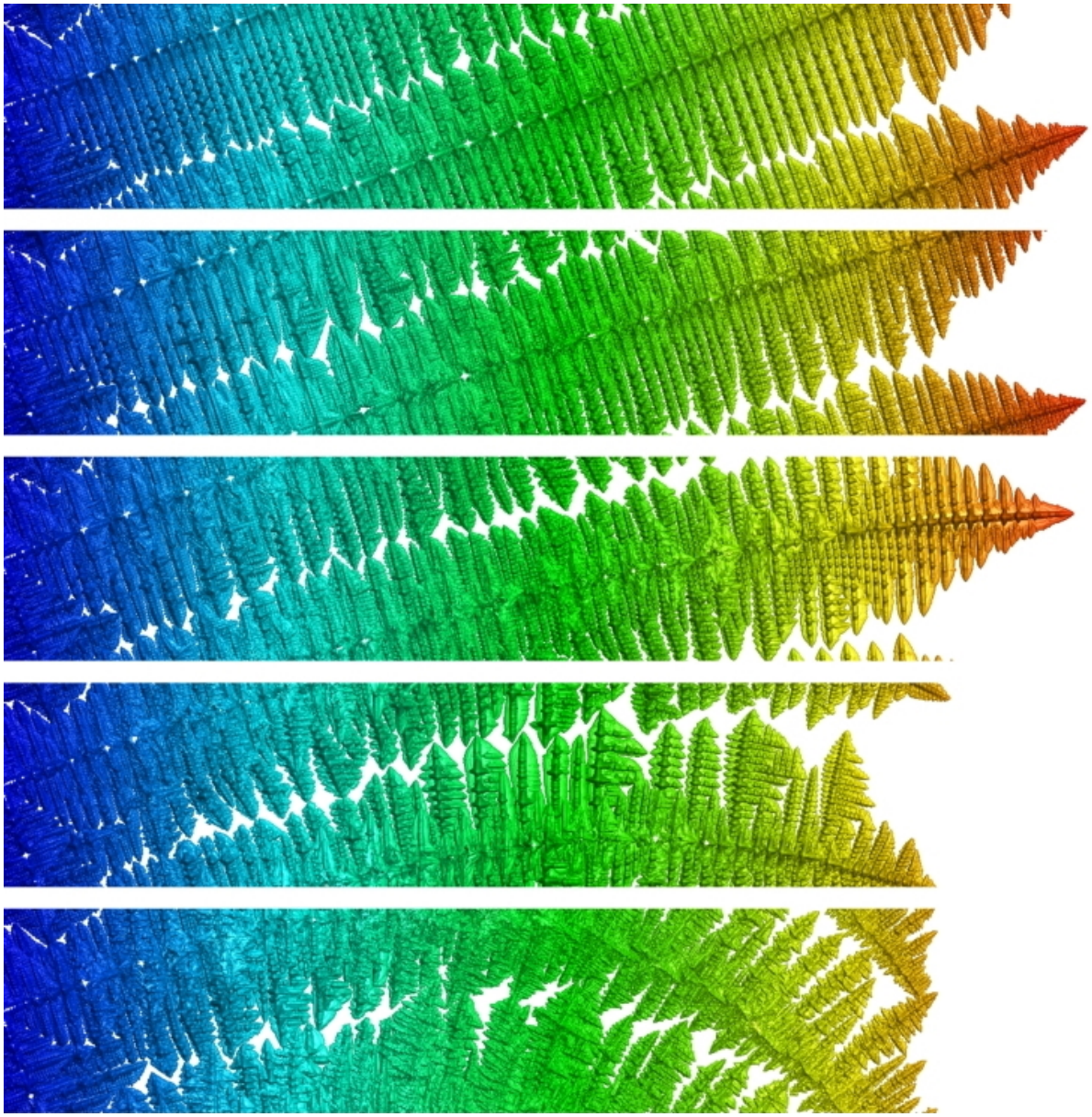

Figure 2: Dendrite structures for cases 1, 10, 25, 50 and 100 in descending order at final time step $t = 250000$.

orientation change. Consequently, the orientation change observed for case 100 seems to be approximately 100 times larger than the orientation observed for case 1, with the intermediate cases behaving in the same manner. For cases 1 and 10 this almost linear relationship between force and orientation change holds for the entire simulation, with very similar behaviour and scaled values being observed. However, the other three cases experiencing larger forces quickly diverge significantly from any linear relationship between force size and orientation change, with this disparity likely being caused by the impact of orientation changes on the morphology of the dendrite which does not significantly impact cases 1 and 10. Up until step 100000 all of the dendrites are morphologically quite similar, as the orientation change has been relatively small even for case experiencing larger forces, but after this point cases 25, 50, and 100 begin to show radically different microstructural developments and hence structural behaviour.

t	(a) Orientation change ($\theta°$)					(b) Accumulated v deformation (µm)				
	1	10	25	50	100	1	10	25	50	100
50000	-0.0364	-0.367	-0.905	-1.85	-3.64	-0.0612	-0.604	-1.50	-3.17	-6.66
100000	-0.132	-1.39	-3.54	-7.38	-14.4	-0.503	-5.49	-13.8	-32.7	-65.1
150000	-0.256	-2.79	-7.33	-17.6	-32.3	-0.998	-11.6	-32.9	-130	-200
200000	-0.383	-4.14	-12.0	-26.9	-60.1	-1.39	-18.9	-57.6	-230	-504
250000	-0.507	-5.49	-18.5	-34.0	-78.1	-2.00	-27.0	-144	-282	-687

Table 2: Comparison of (a) orientation change ($\theta°$) and (b) maximum accumulated v deformation (µm) values for the 5 cases throughout the simulation.

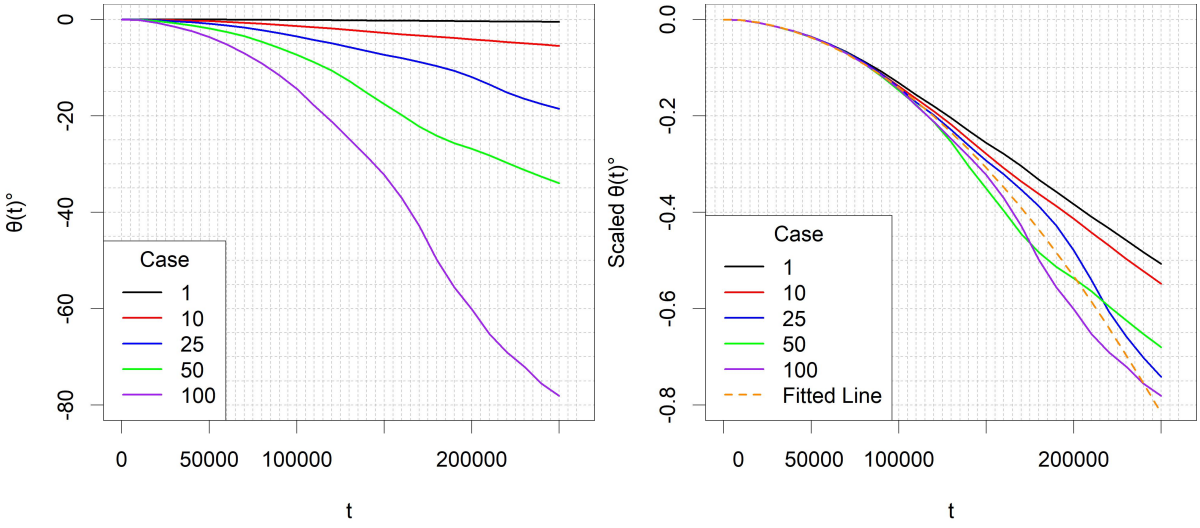

(a) Real values.

(b) Scaled values

Figure 3: Case comparison plots for largest observed orientation change θ at time step t. Scaled orientation change showing full simulation including a fitted power law of $\theta(t) = -4 \times 10^{-11} t^{1.91}$.

When considering the transient orientation change behaviour for the first 100000 steps it can be seen that all cases approximately follow a power law of $\theta(t) = -4 \times 10^{-11} t^{1.91}$, but after this point the orientation change behaviour of all cases stops following this distribution and begins to vary dramatically between cases. The rate of change for cases 1 and 10 becomes essentially linear, this is likely as the dendrites transition from being a generally freely moving dendrite (which could be considered as being analogous to a cantilever beam fixed to a wall) to being limited by interaction with surrounding dendrites. Consequently, a relatively consistently sized region near the tip of the dendrite ahead of the arm interaction remains free for the duration of the simulation, causing the rate of orientation change to become almost constant. In cases 25, 50 and 100 the behaviour after step 100000 becomes more complicated to characterise, with signifiant behavioural differences between cases and no clear fixed pattern. From this point onwards the rate of orientation change both increases and decreases at seemingly unrelated time steps and while the cases using larger forces always have a correspondingly larger orientation change in an absolute sense, when considering the scaled outputs it can been seen that in relative terms the cases experiencing the larger forces do not always correspond to a larger scaled orientation change. For example, if considering the scaled solutions for case 50 this experiences the largest relative orientation changes of all the cases between $t = 125000$ to 175000, yet by the end of the

simulation it has a relative orientation change lower than that observed in case 25. This seems to highlight that predicting the orientation change becomes increasingly difficult in a coupled system once the impact of structural mechanics begins changing the morphology of the dendrite and when interaction with other dendrites begins.

Similar conclusions can be drawn when examining the transient behaviour of the accumulated displacements v across the different cases (the displacements in u and w have been neglected due to being significantly smaller in magnitude, having little impact on microstructure development). The largest accumulated deformation recorded every 50000 time steps can be found in the right half of table 2 and graphs presenting this information at more frequent intervals can be seen in figure 4, again presenting both the real and 'scaled' versions of the data relationships.

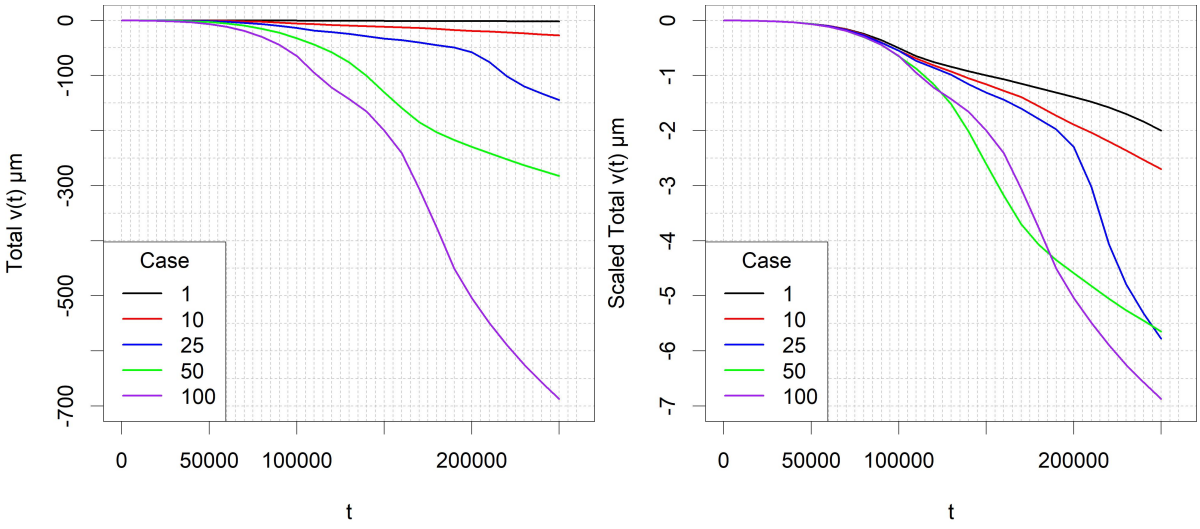

(a) Real values. (b) Scaled values.

Figure 4: Case comparison plots for largest observed cumulative v displacement at time step t.

When considering the transient behaviour of the scaled values in figure 4b, the accumulated behaviour seems to match the general relationships previously described for the orientations, which makes intuitive sense when considering that in this framework the orientation change is a quantity derived from the obtained displacements. Consequently, much as with the orientations, the relative scaled values up to step 100000 are similar for all cases, with cases 1 and 10 remaining similar in behaviour throughout the simulation while the other 3 cases diverge significantly. Considering the real values highlights the non-linear increase in displacement magnitude as the force increases, as when considering cases 1 and 100, the displacements are nearly 350 times larger that those observed in case 1, where a linear relationship would anticipate that they would be approximately 100 times larger.

Finally the maximum step displacement will be examined, which is the single largest v displacement calculated anywhere in the dendrite at a given timestep, to be contrasted with the cumulative displacements considered above which aggregate all the displacements experienced by the dendrite throughout the simulation. Values of this quantity have not been included in a table like the cumulative displacement and orientation as the step displacement has a high variability depending on the state of the system at a given time, such that only by considering the evolution of the step displacements in more granular detail can anything useful be inferred, where graphs of the real an scaled values showing this for all cases throughout the simulation are provided in figure 5.

When considering the scaled values there again seems to be a generally similar step

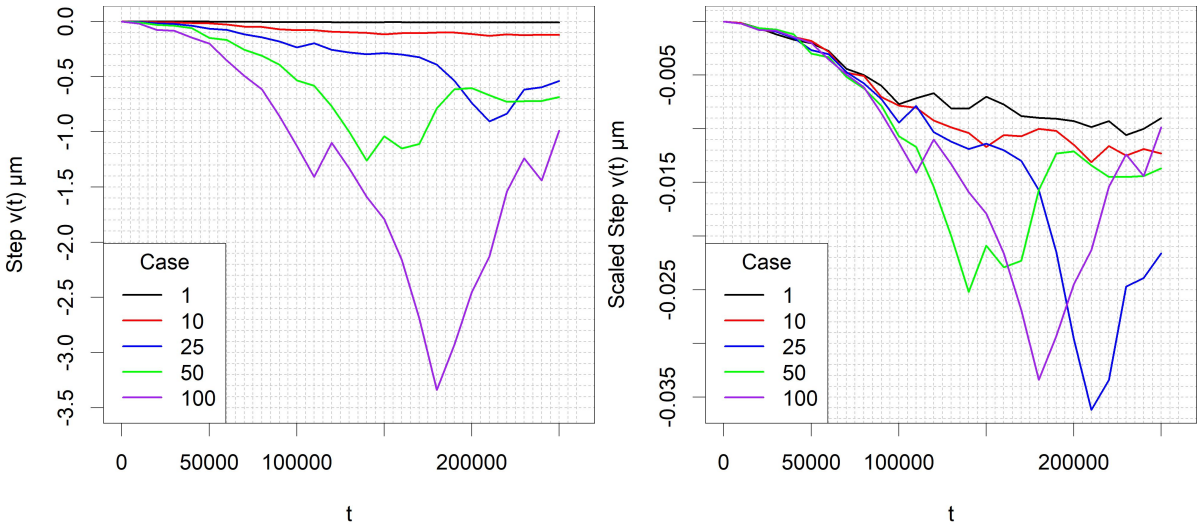

(a) Real values.

(b) Scaled values.

Figure 5: Case comparison plots for largest observed single v displacement at time step t.

displacement behaviour for all cases up to around step $t = 100000$, broadly corresponding with the power law behaviour described when considering the orientation, at which point the behaviour becomes unique for each of the cases. For cases 1 and 10 the step displacements almost plateau off to a constant rate of displacement, with only a slight increase throughout the rest of the simulation. This seems to support the idea that only the region of the tip ahead of the secondary arm interaction is free to move, with this length staying approximately the same for the entirety of the simulation and the slight increase observed is likely due to the small deformations in the growing region constrained by dendrite arm interaction. Case 25 sees a steady increase broadly in line with that observed in cases 1 and 10 until a very sharp increase occurs around $t = 17500$ to 210000, where it obtains the largest observed scaled displacement, at which point the displacements continue to decrease until the end of the simulation (though still having the highest scaled displacement by $t = 250000$). It seems probable that there was a relatively long period where the region near the tip achieved a relatively long length without constriction from secondary arm interaction. This was curtailed significantly around step 210000 as an increasing length of the dendrite becomes constrained by this arm interaction. Case 50 also demonstrates a sharp increase in step displacement between $t = 100000$ and 140000, followed by an equally sharp fall until 190000 at which point the displacements level off to being almost constant. This would again seem to be a case where the altered growth behaviour allows a relatively large region near the tip to remain free ahead of secondary arm interaction for a short period, however once the interaction begins the displacements shrink and become effectively constant due to this free length remaining comparable for the rest of the simulation. For case 100 there is an increase in step displacements until around step $t = 180000$, at which point it beings to decrease at such a precipitous rate that by the end of the simulation even the real step displacement values are comparable to those observed in cases 25 and 50, while the scaled step displacements are comparable to those seen in case 1. This occurs as the tip goes from having the freedom to deform without secondary arm interaction before experiencing this along almost the entire length of the dendrite, finally having the tip become trapped by the end of the simulation. Here the microstructure of the system changes from a free dendrite to an almost continuous block with a significantly lower capacity for displacement.

The assumption made in the literature treating a columnar dendrite as a structure analogous

to a cantilever beam is generally reasonable when considering the behaviour of a single dendrite at a single point in time. However, this study highlights the limitations of this assumption in more realistic scenarios where structural mechanics and microstructure solidification are being resolved concurrently such that the growth behaviour of the microstructure is altered. The cantilever analogy holds broadly true for growing dendrites while they don't experience significant orientation changes and are free from interaction with other dendrites, such as could be observed in approximately the first 100000 steps of all cases. However, even in cases 1 and 10 where orientation changes are relatively small, the simulations still reach a point of secondary arm interaction where only the small region ahead of the arm interaction is free to behave like a beam. As this free region stays approximately the same length for the duration of the simulation, while the behaviour of this region at any given step is similar to that of a deforming beam, the transient displacements essentially progress at a constant rate. For the cases experiencing larger forces, aside from the still existing issue of secondary arm interaction limiting beam like behaviour, these cases will ultimately grow into a structure with a more complex curved morphology that makes any comparisons with a cantilever beam increasingly dubious.

4. Conclusion

A parametric study was undertaken varying the constant body force applied to a solidifying system using a coupled CA solidification and Finite Volume structural mechanics solver. The varying force was found to significantly alter both the growth behaviour and final morphology of the solidifying dendritic system. These results were then considered in the context of the analogy of cantilever beam-like structural behaviour when describing the mechanical behaviour of columnar dendrite. While this analogy can be helpful for understanding the behaviour of a single dendrite, it generally fails to describe the transient dynamics of the true interdependent system, which requires fully coupled modelling to truly understand the behaviour even for relatively simple cases such as those examined here.

Acknowledgments

Acknowledgments P.S. gratefully acknowledges the financial assistance offered by the University of Greenwich VC scholarship for his PhD studies which provided the foundation for this work.

References

[1] Reinhart G, Nguyen-Thi H, Mangelinck-Noël N, Baruchel J and Billia B 2014 *JOM* **66** 1408–1414
[2] Ananiev S, Nikrityuk P and Eckert K 2009 *Acta Mater.* **57** 657–665
[3] Aveson J, Tennant P, Foss B, Shollock B, Stone H and D'Souza N 2013 *Acta Mater.* **61** 5162–5171
[4] Hu S, Liu L, Yang W, Sun D, Huo M, Huang T, Zhang J, Su H and Fu H 2019 *Metall. Mater. Trans. A* **50** 1607–1610
[5] Hallensleben P, Scholz F, Thome P, Schaar H, Steinbach I, Eggeler G and Frenzel J 2019 *Crystals* **9** 149
[6] Takaki T and Kashima H 2011 *J. Cryst. Growth* **337** 97–101
[7] Aveson J, Reinhart G, Nguyen-Thi H, Mangelinck-Noël N, d'Souza N and Stone H 2014 *MATEC Web of Conferences* vol 14 (EDP Sciences) p 05003
[8] Sun D, Liu L, Huang T, Yang W, Li Y, Yue Q, Zhang J and Fu H 2018 *Prog. Nat. Sci.: Mater. Int.* **28** 489–495
[9] Huo M, Liu L, Yang W, Hu S, Sun D, Su H, Zhang J and Fu H 2019 *Vacuum* **161** 29–36
[10] Billia B, Bergeon N, Thi H N, Jamgotchian H, Gastaldi J and Grange G 2004 *Phys. Rev. Lett.* **93** 126105
[11] Chen C, Sun J, Diao A, Yang Y, Li J and Zhou Y 2022 *J. Alloys Compd.* **891** 161949
[12] Yamaguchi M and Beckermann C 2013 *Acta Mater.* **61** 4053–4065
[13] Soar P, Kao A, Djambazov G and Pericleous K 2022 *JOM* 1–9
[14] Soar P, Kao A, Shevchenko N, Eckert S, Djambazov G and Pericleous K 2022 *Philos. Trans. R. Soc. London, Ser. A* **380** 20210149
[15] Wang W, Lee P D and Mclean M 2003 *Acta Mater.* **51** 2971–2987
[16] Kao A, Krastins I, Alexandrakis M, Shevchenko N, Eckert S and Pericleous K 2019 *JOM* **71** 48–58